Time domain approaches to the stability analysis of flexible dynamical systems*

Jielong Wang, Xiaowen Shan and Bin Wu
Beijing Aeronautical Science & Technology Research Institute,
Commercial Aircraft Corporation of China, Ltd.
Beijing 102211, PR China
Olivier A. Bauchau
University of Maryland, Department of Aerospace Engineering,
College Park, MD 20742, USA

Abstract

The paper presents two approaches to the stability analysis of flexible dynamical systems in the time domain. The first is based on the partial Floquet theory and proceeds in three steps. A preprocessing step evaluates optimized signals based on the proper orthogonal decomposition method. Next, the system stability characteristics are obtained from partial Floquet theory through singular value decomposition. Finally, a postprocessing step assesses the accuracy of the identified stability characteristics. The Lyapunov characteristic exponent theory provides the theoretical background for the second approach. It is shown that the system stability characteristics are related to the Lyapunov characteristic exponent closely, for both constant and periodic coefficient systems. For the latter systems, an exponential approximation is proposed to evaluate the transition matrix. Numerical simulations show the proposed approaches are robust enough to deal with the stability analysis of flexible dynamical systems and the predictions of the two approaches are found to be in close agreement.

1 Introduction

Static and dynamic instabilities, such as divergence, flutter, or buckling, are ever present concerns for the aerospace industry. Buckling is a purely mechanical phenomenon, whereas flutter and divergence are aeroelastic phenomena. Flutter analysis has become an indispensable step in the design of commercial aircraft. The p and U-g methods, both based on linearized governing equations with constant coefficients, are widely used to evaluate the damping of the system and assess its stability. The systematic use of composite materials enables the design of longer, more flexible wings resulting in larger tip deflections under load. For such systems, nonlinear behavior becomes an issue and the use of the traditional p and U-g methods becomes questionable. When dealing with rotating systems, additional types of instabilities, such as whirl flutter, could occur. In this case, the governing equations feature periodic coefficients, which the p and U-g method are not equipped to handle. This paper presents two time domain approaches to stability analysis, the modified partial Floquet and Lyapunov characteristic exponent methods, which can both handle constant and periodic coefficient systems in an efficient manner.

* *Journal of Computational and Nonlinear Dynamics*, **11**(4): 041003 (9 pages), 2016

Floquet theory [1, 2] is a powerful tool for the analysis of periodic systems. Stability characteristics can be extracted from the *transition matrix*. Unfortunately, the computational cost associated with the evaluation of the transition matrix becomes overwhelming when dealing with large-scale models and hence, application of Floquet theory has been limited to the investigation of small-size systems. While the detailed analysis of complex systems requires large-dimensional models, it is often the case that the physical phenomena causing the instability involve a small number of degrees of freedom only. Therefore, the identification of the few dominant eigenvalues of the transition matrix from a minimal set of output signals of the system could provide enough information to assess its stability characteristics. For instance, Wang [3] developed an approach based on partial Floquet theory while Bauchau and Wang [4, 5] used the Prony and Snapshot methods. These approaches require time series of the system's dynamic response only. Hence, they can be used to assess stability characteristics in both experimental and numerical settings. This paper presents first a modification of the partial Floquet theory, which combines it with the Proper Orthogonal Decomposition (POD) and Singular Value Decomposition (SVD) techniques to improve its robustness and efficiency.

The evaluation of the Lyapunov Characteristic Exponents (LCEs) [6, 7] is a well established approach to stability analysis. These exponents were introduced by Lyapunov in the context of non-stationary solutions of ordinary differential equations. They characterize the asymptotic behavior of nonlinear dynamical systems by giving a measure of the exponential growth or decay of small perturbations about a nominal trajectory. Because LCEs measure the sensitivity of solutions of dynamical systems to small perturbations, they are often used as stability indicators for periodic and chaotic systems.

Unfortunately, for large-scale systems, the evaluation of the LCEs entails a heavy computational penalty, hindering their widespread use for stability analysis. In this paper, the linearized governing equations of the system are projected onto the modal subspace defined by its dominant eigenvalues and the LCEs are then extracted at a far lower computational cost.

In the second approach, the LCEs are evaluated to assess the stability characteristics of numerical models with constant or periodic coefficients. First, a nominal trajectory is determined through the integration of the nonlinear governing equations of motion. Next, the system is linearized about this nominal trajectory and the dominant eigenvalues of this linearized system are extracted. For systems with constant coefficients, these eigenvalues are identical to the stability characteristics and their real parts equal the LCEs. For systems with periodic coefficients, the linearized equations are projected onto the modal space defined by the eigenmodes associated with the dominant eigenvalues, providing an approximation to the Floquet transition matrix; the LCEs are the real parts of the Floquet characteristic exponents. Because linearization is used, the proposed approach to stability analysis is limited to systems presenting weak nonlinearities. Only the dominant eigenmodes are used and the transition matrix is evaluated through an exponential approximation.

This paper presents two approaches to the efficient stability analysis of dynamical systems. For both approaches, the stability characteristics of nonlinear systems are obtained from time domain simulations only. The first approach is based on partial Floquet theory and combines it with POD and SVD techniques to achieve efficiency and reliability. The second approach is based on the theory of LCEs. An exponential approximation is proposed evaluate the Floquet transition matrix, providing an efficient and robust estimate of the system stability characteristics.

Section 2 describes the partial Floquet approach. Section 3 provides the background about the LCEs and details the procedure used to evaluate them. Section 4 validates the proposed approaches by means of two numerical examples.

2 Robust approach for stability analysis

The stability analysis procedure developed by Bauchau and Wang [8] is enhanced to improve its efficiency and robustness. In the current approach, POD is performed at the onset of the process to filter out signal noise. Next, the partial Floquet analysis is applied to identify the system's frequency and damping characteristics from the filtered signals. Finally, curve fitting techniques are used to reconstruct the signals based on the identified characteristics. The discrepancy between the original and reconstructed signals is used as an accuracy indicator.

2.1 Governing equations of motion

Without loss of generality, the governing equations of motion [9, 10] for flexible dynamical systems can be written as a set of ordinary differential equations

$$\underline{\underline{M}}\,\underline{\ddot{q}} = \underline{F}(\underline{q}, \underline{\dot{q}}), \tag{1}$$

where $\underline{\underline{M}}$ is the mass matrix; array $\underline{q}$, of size N, stores the displacement components, array $\underline{F}(\underline{q}, \underline{\dot{q}})$ stores all other elastic and dynamics forces. First and the second order time derivatives are indicated as $\dot{(\cdot)}$ and $\ddot{(\cdot)}$, respectively.

To perform the stability analysis, governing equations (1) are linearized about an equilibrium point and recast into a homogeneous state space form,

$$\underline{\dot{u}}(t) = \underline{\underline{A}}\,\underline{u}(t). \tag{2}$$

The following notation was introduced

$$\underline{\underline{A}} = \begin{bmatrix} 0 & \underline{\underline{I}} \\ -\underline{\underline{M}}^{-1}\underline{\underline{K}} & -\underline{\underline{M}}^{-1}\underline{\underline{C}} \end{bmatrix}, \quad \underline{u}(t) = \begin{Bmatrix} d\underline{q} \\ d\underline{\dot{q}} \end{Bmatrix}, \tag{3}$$

where $\underline{\underline{K}}$ and $\underline{\underline{C}}$ are the stiffness and damping matrices of the linearized system, respectively, $d(\cdot)$ indicates small perturbations in the variable, and matrix $\underline{\underline{I}}$ is the identity matrix. The size of the system of state space equations is $m = 2N$.

2.2 Proper orthogonal decomposition

The governing equations of motion (1) are solved numerically at discrete time steps $t_k = k\Delta t$, where Δt is the time step size. Let array $\underline{u}_k$ store the computed response of the system at time t_k, *i.e.*, $\underline{u}_k = \underline{u}(k\Delta t)$. Due to the space and time discretization processes and to round-off errors, this highly redundant data set is corrupted with noise. As a preprocessing step, Bauchau and Wang [8] proposed to use the POD technique, which filters out noise and reduces the size of the data considerably.

The response matrix is assembled from the computed time histories as $\underline{\underline{T}}_0 = \left[\underline{u}_0, \underline{u}_1, \ldots, \underline{u}_{n-1}\right]$. The proper orthogonal modes, stored as the columns of matrix $\underline{\underline{U}}$, are obtained from a singular value decomposition the response matrix: $\underline{\underline{T}}_0 = \underline{\underline{U}}\,\underline{\underline{\Sigma}}\,\underline{\underline{V}}^T$, where matrices $\underline{\underline{U}}$ and $\underline{\underline{V}}$ are orthogonal and diagonal matrix $\underline{\underline{\Sigma}} = \mathrm{diag}(\sigma_i)$ stores the singular values [11]. Because the data stored in the response matrix is highly redundant, only a few singular values dominate and the singular value decomposition is truncated to a user determined rank number r, *i.e.*, $\underline{\underline{T}}_0 \approx \underline{\underline{U}}_r\,\underline{\underline{\Sigma}}_r\,\underline{\underline{V}}_r^T$. The linearized system (2) is projected onto the subspace of the r dominant proper orthogonal modes,

$$\underline{\dot{\hat{u}}}(t) = \underline{\underline{\hat{A}}}\,\underline{\hat{u}}(t), \tag{4}$$

where the reduced system matrix is $\underline{\underline{\hat{A}}}_{(r\times r)} = \underline{\underline{U}}_r^T\,\underline{\underline{A}}\,\underline{\underline{U}}_r$ and $\underline{\hat{u}}(t) = \underline{\underline{U}}_r^T\,\underline{u}(t)$.

The r generalized or optimal signals, $\underline{h}_i$, are extracted from the projected response of the system,

$$\underline{h}_i = \sigma_i \underline{v}_i, \quad i = 1, 2, \ldots, r \tag{5}$$

where $\underline{v}_i$ the i^{th} column of $\underline{\underline{V}}_r$. The generalized signals are mutually orthogonal and contain most of the energy of the system.

2.3 Partial Floquet theory

Once the generalized signals are obtained, the stability characteristics of the linearized system, eq. (2), can be identified with the help of the partial Floquet theory. The *output Hankel matrices*, $\underline{\underline{H}}_1$ and $\underline{\underline{H}}_0$, store combinations of generalized signals, $\underline{h}_i$. For instance, the columns of matrix $\underline{\underline{H}}_0$ consist of n_s arrays,

$$\underline{\underline{H}}_0 = \left[\underline{h}_i, \underline{h}_{i+p}, \ldots, \underline{h}_{i+(n_s-1)p}\right], \tag{6}$$

where arrays $\underline{h}_{i+jp}$ store m_s consecutive data points of optimized signal $\underline{h}_i$ starting at the j^{th} period. Matrix $\underline{\underline{H}}_1$ is identical to matrix $\underline{\underline{H}}_0$, but the date is shifted by one period; more details are given by Bauchau and Wang [8].

The Floquet transition matrix, $\underline{\underline{Q}}$, relates these two Hankel matrices, $\underline{\underline{H}}_1 = \underline{\underline{Q}}\,\underline{\underline{H}}_0$. Because matrix $\underline{\underline{H}}_0$ contains highly redundant data, the transition matrix cannot be evaluated exactly. The Moore-Penrose inverse [11] of $\underline{\underline{H}}_0$ is evaluated using the singular value decomposition as $\underline{\underline{H}}_0^+ = \underline{\underline{V}}_{0r}\underline{\underline{\Sigma}}_{0r}^{-1}\underline{\underline{U}}_{0r}^T$, providing an estimate of the transition matrix,

$$\underline{\underline{\hat{Q}}}_{(r\times r)} = \underline{\underline{U}}_{0r}^T \underline{\underline{H}}_1 \underline{\underline{V}}_{0r} \underline{\underline{\Sigma}}_{0r}^{-1}. \tag{7}$$

The stability characteristics of the system are then extracted from the eigenvalues of the approximate transition matrix. The eigenvalues of the transition matrix $\hat{Q}$, referred to as "Floquet characteristic exponents" and denoted λ_j, are written as $\exp(\lambda_j T) = r_j \exp(\pm \mathbf{i}\phi_j)$, where $\mathbf{i} = \sqrt{-1}$ and T the period of the system. It follows that $\lambda_j = \omega_j[\zeta_j \pm \mathbf{i}(1-\zeta_j^2)^{1/2}]$, where ω_j and ζ_j are the frequency and damping parameters, respectively, associated with this characteristic exponent and hence,

$$\zeta_j = \frac{c_j}{\sqrt{1+c_j^2}}, \quad \omega_j = \frac{\phi_j}{T}\sqrt{1+c_j^2}, \tag{8}$$

where $c_j = (\ln r_j)/\phi_j$ for $j = 1, 2, \ldots, r$.

2.4 Error estimation

Because the data is noisy, the partial Floquet theory may lead to inaccurate estimates of system characteristics. A post-processing procedure is used to estimate the error. Based on the identified system characteristics the generalized signals are reconstructed [8] and the discrepancy between the original and reconstructed signals is used as an error estimate

$$\epsilon = \sqrt{\frac{1}{n}\sum_{k=1}^{n}(h_{k,\ell} - \hat{h}_{k,\ell})^2}, \tag{9}$$

where $h_{k,\ell}$ and $\hat{h}_{k,\ell}$ are the original and reconstructed signals, respectively, and n is the total number of sampling points. If ϵ is small, the reconstructed signals approximate the original signals closely, implying a reliable estimate of system characteristics.

3 Eigenvalue decomposition based approach

The proposed stability analysis approach based on LCEs is described in this section. The concept of LCEs provides a theoretical foundation of the approach while modal reduction improves its efficiency.

3.1 Definition of the LCEs

By definition, the fundamental matrix solution, denoted $\underline{\underline{U}}(t)$, of linearized system (2) satisfies these equations,

$$\dot{\underline{\underline{U}}}(t) = \underline{\underline{A}}\,\underline{\underline{U}}(t),\ \underline{\underline{U}}(0) = \underline{\underline{I}}. \tag{10}$$

Assuming regularity conditions to be satisfied [6], the LCEs, denoted ρ_j, are defined as follows,

$$\rho_j = \lim_{t\to\infty} \frac{\ln \alpha_j(t)}{2t}, \quad j = 1, 2, \ldots, m, \tag{11}$$

where $\alpha_j(t)$ are the eigenvalues of the matrix $\underline{\underline{U}}^T(t)\underline{\underline{U}}(t)$.

The LCEs determine the asymptotic behavior of the dynamical system. If the largest LCE is negative, the system evolves to a fixed point or a stable periodic orbit; the system is nonconservative and exhibits asymptotic stability. If the largest LCE vanishes, the system is neutrally stable. Finally, if the largest LCE is positive, the system is chaotic and unstable.

If matrix $\underline{\underline{A}}$ is constant, an explicit form of the fundamental matrix solution exists,

$$\underline{\underline{U}}(t) = \exp(\underline{\underline{A}}t)\underline{\underline{U}}(0) = \underline{\underline{\Phi}}\exp(\underline{\underline{\Lambda}}t)\underline{\underline{\Phi}}^{-1}, \tag{12}$$

where the diagonal matrix $\underline{\underline{\Lambda}}$ and matrix $\underline{\underline{\Phi}}$ store the eigenvalues and eigenvectors of matrix $\underline{\underline{A}}$, respectively, *i.e.*, $\underline{\underline{A}} = \underline{\underline{\Phi}}\,\underline{\underline{\Lambda}}\,\underline{\underline{\Phi}}^{-1}$. Based on eq. (11), it can be shown that the LCEs are identical to the real parts of the eigenvalues of matrix $\underline{\underline{A}}$.

If matrix $\underline{\underline{A}}$ is periodic, *i.e.*, $\underline{\underline{A}}(t+T) = \underline{\underline{A}}(t)$, the Floquet transition matrix is obtained by integration over one period,

$$\underline{\underline{Q}} = \underline{\underline{U}}(T). \tag{13}$$

The LCEs are the real parts of the Floquet characteristic exponents, $\rho_j = \omega_j\zeta_j$. Note that ω_j and ζ_j are quantities associated with the eigenvalues of the transition matrix; they are not the frequency and damping characteristics of the system.

3.2 Computation of the LCEs

Periodic systems only are discussed here, because constant coefficient systems are a special case of periodic systems with an arbitrary period. In principle, the determination of LCEs proceeds as follows: *(1)* compute of a fiducial trajectory by solving the nonlinear equations of motion, eqs. (1), *(2)* evaluate the fundamental matrix solution, $\underline{\underline{U}}(T)$, by solving linearized system (2), and *(3)* extract the LCEs from matrix $\underline{\underline{U}}(T)$ using eq. (11). Clearly, this approach carries a heavy computational burden as the problem size increases. The main contribution of this work is the development of an alternative, computationally efficient approach.

First, the Arnoldi algorithm [12] is used to extract the dominant eigenvalues of system (2) and the corresponding eigenvectors are stored in matrix $\underline{\underline{\hat{\Phi}}}$. It is not necessary to extract more than a few dominant eigenvalues, because the remaining ones have no impact on stability. For systems with constant coefficients, the identified natural frequency and damping characteristics of the system can be used for stability assessment directly.

For periodic systems, system (2) is projected onto the subspace associated with the dominant eigenvalues to find

$$\dot{\underline{\bar{u}}}(t) = \underline{\underline{\bar{A}}}\,\underline{\bar{u}}(t) \tag{14}$$

where $\underline{\bar{u}} = \underline{\underline{\hat{\Phi}}}^T \underline{u}$ and $\underline{\underline{\bar{A}}} = \underline{\underline{\hat{\Phi}}}^T \underline{\underline{A}}\,\underline{\underline{\hat{\Phi}}}$. The fundamental matrix solution of the reduced model, $\underline{\underline{\bar{U}}}(t)$, is obtained from eq. (14) with the initial condition $\underline{\underline{\bar{U}}}(0) = \underline{\underline{I}}$. For reasons of convergence and accuracy, the time step size, Δt, used for the solution of the nonlinear equations of motion is small and it is reasonable to assume matrix $\underline{\underline{\bar{A}}}$ to remain constant within each time step. In view of eq. (12), an approximate solution of reduced problem (14) is then

$$\underline{\underline{\bar{U}}}(T) \approx \exp(\sum_{i=1}^{p} \underline{\underline{\bar{A}}}_{p-i} \Delta t)\underline{\underline{\bar{U}}}(0) \tag{15}$$

where $\underline{\underline{\bar{A}}}_i = \underline{\underline{\bar{A}}}(i\Delta t)$ and $p = T/\Delta t$ is the number of sampling points per period.

Numerous algorithms [7, 13] have been proposed to evaluate the LCEs of a system. The proposed approach uses the exponential approximation (15), which reveals the close relationship between the LCEs and frequency and damping characteristics of the system. Because the size of the system has been reduced considerably, the computational cost associated with eq. (15) is low.

In summary, the proposed approach LCE proceeds as follows: *(1)* obtain a fiducial trajectory by integrating the nonlinear equations of motion, *(2)* extract the dominant eigenvalues of system (2) using the Arnoldi algorithm [12], *(3)* extract the eigenvalues of $\underline{\underline{\bar{A}}}_i$ at discrete times $i\Delta t$ for $i = 0, 1, \ldots, p-1$, (4) estimate $\underline{\underline{\bar{U}}}(T)$ using the exponential approximation (15), and finally, *(5)* determine the LCEs as the eigenvalues of matrix $\underline{\underline{\bar{U}}}(T)$.

3.3 Eigenvalue decomposition procedure

The proposed approach calls for the extraction of the dominant eigenvalues of the system. The governing equations (1) define the following generalized eigenproblem

$$(\lambda_j^2 \underline{\underline{M}} + \lambda_j \underline{\underline{C}} + \underline{\underline{K}})\underline{\phi}_j = \underline{0}, \tag{16}$$

where $(\lambda_j, \underline{\phi}_j)$ are the eigenpairs.

In dynamical systems, singular stiffness matrices are often encountered due to the presence of rigid body modes. To circumvent this problem, the eigenproblem is shifted by a positive quantity μ,

$$(\breve{\lambda}_j^2 \underline{\underline{\breve{M}}} + \breve{\lambda}_j \underline{\underline{\breve{C}}} + \underline{\underline{\breve{K}}})\underline{\phi}_j = \underline{0}, \tag{17}$$

where $\underline{\underline{\breve{M}}} = \underline{\underline{M}}$, $\underline{\underline{\breve{C}}} = \underline{\underline{C}} - 2\mu\underline{\underline{M}}$, $\underline{\underline{\breve{K}}} = \underline{\underline{K}} - \mu\underline{\underline{C}} + \mu^2\underline{\underline{M}}$ and the eigenvalue has been shifted by μ, $\lambda_j = \breve{\lambda}_j - \mu$. Because matrix $\underline{\underline{\breve{K}}}$ is always invertible, the eigenproblem is recast as

$$\underline{\underline{\mathcal{A}}}\,\underline{p}_j = \breve{\rho}_j \underline{p}_j, \tag{18}$$

where

$$\underline{\underline{\mathcal{A}}} = \begin{bmatrix} -\underline{\underline{\breve{K}}}^{-1}\underline{\underline{\breve{C}}} & -\underline{\underline{\breve{K}}}^{-1}\underline{\underline{\breve{M}}} \\ \underline{\underline{I}} & \underline{\underline{0}} \end{bmatrix},\ \underline{p}_j = \begin{Bmatrix} \underline{\phi}_j \\ \breve{\lambda}_j \underline{\phi}_j \end{Bmatrix},\ \breve{\rho}_j = \frac{1}{\breve{\lambda}_j}. \tag{19}$$

For complex conjugates eigenvalues, $\lambda_j = \Re(\lambda_j) \pm \mathbf{i}\ \Im(\lambda_j)$, the associated frequency and damping characteristics of the system are

$$\omega_j = \sqrt{\Re^2(\lambda_j) + \Im^2(\lambda_j)}, \quad \zeta_j = \Re(\lambda_j)/\omega_j \tag{20}$$

4 Numerical simulation

Two numerical examples are presented in this section to validate the proposed stability analysis procedure.

4.1 Flutter of Goland wing

The first example deals with the flutter problem of the rectangular planform Goland [14] wing. The wing's geometry is as follows: half-wing length is $L = 20$ ft and chord length $c = 6$ ft. The airfoil quarter-chord and center of mass are located 0.5 and 0.6 ft aft the elastic axis of the wing, respectively. The physical properties are: bending stiffness, $EI = 2.365 \times 10^7$ lbs·ft^2, torsional stiffness, $GJ = 2.390 \times 10^6$ lbs·ft^2, mass per unit span, $m = 0.746$ slugs/ft, polar moment of inertia, $I = 1.947$ slugs·ft. A more detailed description of the configuration can be found in Goland [14].

Figure 1 shows the wing in its reference and deformed configurations: under the effects of the aerodynamic loads, the wing bends and twists. At the same time, the deformation of the wing redistributes the aerodynamic loading. When the flow speed reaches 590 ft/s, wind tunnel tests show that flutter results from this aeroelastic interaction.

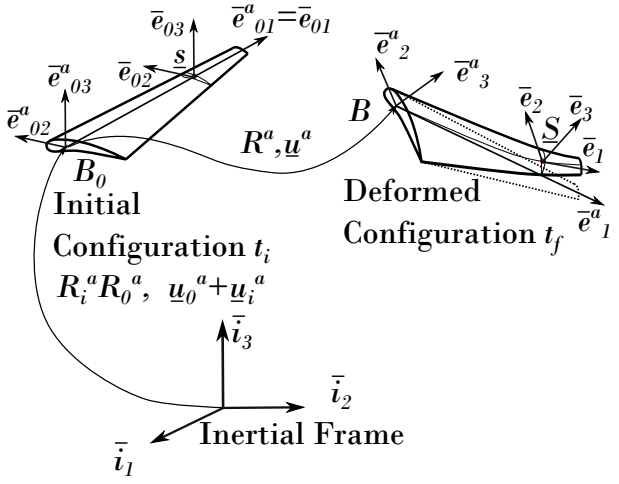

Figure 1: Motion of the wing under aerodynamic load

The structural model consists of a revolute joint that connects the root of the wing to the ground and of a flexible wing. Due to symmetry, only half of the system is modeled. The flexible wing is modeled with geometrically exact beam elements [9, 15]; four cubic finite elements were used to model the wing. By prescribing the relative rotation at the revolute joint, the wing's angle of attack can be modified.

The aerodynamic model relies on the modified strip theory [16, 17] that estimates the aerodynamic lift, P_a, and pitching moment about the elastic axis, M_a, both per unit length of the wing, through the following expressions,

$$\begin{aligned} P_a =& - C_{\ell\alpha,n}\rho v_n b C_T\ Q - \pi\rho b^2[\ddot{h} + v_n\dot{\theta}] + \pi\rho b^3 a\ddot{\theta}, \\ M_a =& - \pi\rho b^4(\frac{1}{8} + a^2)\ddot{\theta} + \pi\rho b^3 a\ddot{h} \\ & + \pi\rho v_n b^2\dot{h} + \pi\rho v_n^2 b^2\theta \\ & - 2\pi\rho v_n b^2[\frac{1}{2} - (a - ac_n)C_T\frac{C_{\ell\alpha,n}}{2\pi}]Q, \end{aligned} \tag{21}$$

where Q is the downwash defined as

$$Q = -\dot{h} + v_n\theta + b(\frac{C_{\ell\alpha,n}}{2\pi} + ac_n - a)\dot{\theta}, \tag{22}$$

and C_T a wake associated function. Both Theodorsen [18] and Scherer [19, 20] provide approximations for this function; the latter expression is used here,

$$C_T(k_n) = \frac{\mathcal{A}\!\mathcal{R}}{2 + \mathcal{A}\!\mathcal{R}}C_J(k_n) \tag{23}$$

where $\mathcal{R}$ is the wing's aspect ratio, $k_n = \omega b/v_n$ is the reduced frequency, ω the wing's oscillation frequency, and the complex function $C_J(k_n) = F_J(k_n) + \mathbf{i}\ G_J(k_n)$. Scherer provides the following approximations: $F_J(k_n) = 1 - a_1 k_n^2/(k_n^2 + a_2^2)$ and $G_J(k_n) = -a_1 a_2 k_n/(k_n^2 + a_2^2)$ where $a_1 = 0.5\mathcal{R}/(2.32 + \mathcal{R})$ and $a_2 = 0.181 + 0.772/\mathcal{R}$. If the unsteady motion of the wing is assumed to be harmonic, $\dot{Q} = \mathbf{i}\omega Q$ and the complex product $C_T Q = \mathcal{R}(F_J\ Q + G_J \dot{Q}/\omega)/(2 + \mathcal{R})$.

All the other symbols appearing in the expression of aerodynamic lift and moment are as follows: $C_{\ell\alpha,n}$ is the local lift curve slope for a wing section perpendicular to the elastic axis in steady flow, ρ the air density, v_n the air stream velocity perpendicular to elastic axis, b the wing's semi-chord length measured perpendicular to the elastic axis, h the heaving of the wing's elastic axis, θ the wing's local twist about the elastic axis, a the non-dimensional distance from mid-chord to elastic axis, and ac_n the non-dimensional distance from mid-chord to local aerodynamic center measured perpendicular to the elastic axis.

The input parameters for the aerodynamic models were selected as: reduced frequency $k_n = 0.16$, air density $\rho = 2.1881 \times 10^{-3}$ slugs/ft^3, the local lift curve slope $C_{\ell\alpha,n} = 6.2832$, aspect ratio $\mathcal{R} = 3.333$, and $a = ac_n = -0.5$. The air flow velocity is $v_n \in [300, 700]$ ft/s.

The Radau IIA type implicit solver [21] was used to simulate the dynamic response of the complete system with a user defined tolerance $\tau_a = 1 \times 10^{-3}$. The root angle of attack is prescribed as $\theta_a = 0.15 - 0.15\cos(10\pi\ t)$ for $0 \le t \le 0.2$ s and $\theta_a = 0$ for $t \ge 0.2$ s. The response of the system is simulated for 1 s, providing the reference trajectory. Two approaches were used to evaluate the stability characteristics: the partial Floquet and the LCEs approaches.

For the partial Floquet approach, six optimized signals were extracted from the computed response for $t \in [0.2, 1]$ s using POD. For the LCEs approach, the system is assumed to feature constant coefficients. Eigenvalues of the linearized system are extracted during the dynamic simulation and the time averaged eigenvalues are used to identify the flutter modes. It is not necessary to extract the eigenvalues of the linearized system at each time step of the dynamic simulation. In this example, eigenvalue analysis was performed at every 3 time steps to further lower computational cost.

Table 1: Mean value of the stability characteristics

Mode i	1	2	3	4
ω_i	61.76	70.11	236.5	335.3
ζ_i	- 33.60	- 7.794	- 9.050	- 2.317

Figure 2 shows the stability characteristics of the first four modes obtained with the LCEs approach for a far field flow velocity $v_n = 500$ ft/s. Because the deformation of the wing remains small during the entire simulation, the stability characteristics remain nearly constant for $t \in [0, 0.6]$ s and eventually converge to the time averaged quantities shown in Table 4.1.

Next, the stability characteristics versus far field flow velocity predicted by the two approaches are compared in fig. 3. The flutter speeds predicted by the two approaches are found to be in close agreement: $U_F = 586$ and 588 ft/s for the partial Floquet and LCEs approaches, respectively. The experimentally measured flutter speed [14] is 590 ft/s. For far field flow velocities in excess of the flutter speed, the system is unstable and the wing elastic displacements become large, resulting in strong nonlinearities in both structural and aerodynamic models. The stability characteristics predicted by both approaches start to diverge because the assumptions on which they are based are violated.

In the partial Floquet approach, stability characteristics are extracted from optimized signals, as discussed in section 2.3. To check the accuracy of this process, the signals are reconstructed based on the identified stability characteristics and error measure (9) quantifies the discrepancy

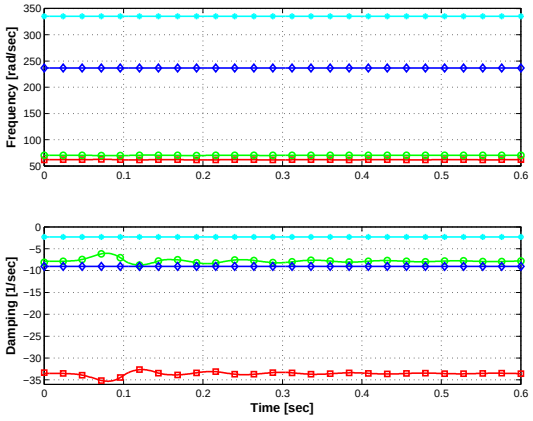

Figure 2: Frequency (top figure) and damping (bottom figure) characteristics ($v_n = 500$ ft/s). Mode 1 ($\square$), 2 ($\circ$), 3 ($\diamond$), and 4 ($*$).

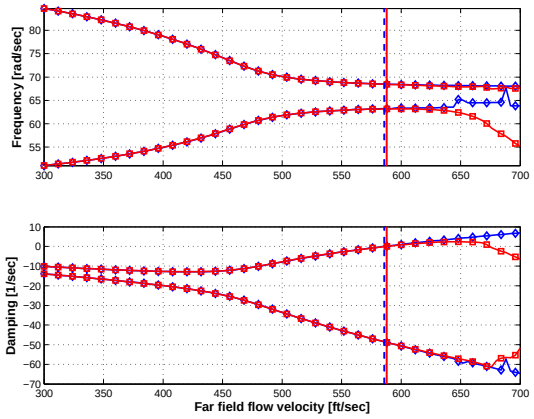

Figure 3: Stability characteristics versus far field flow velocity for the partial Floquet ($\diamond$) and LCEs ($\square$) approaches. Predicted flutter boundary: partial Floquet (dashed vertical line) and LCEs (solid vertical line).

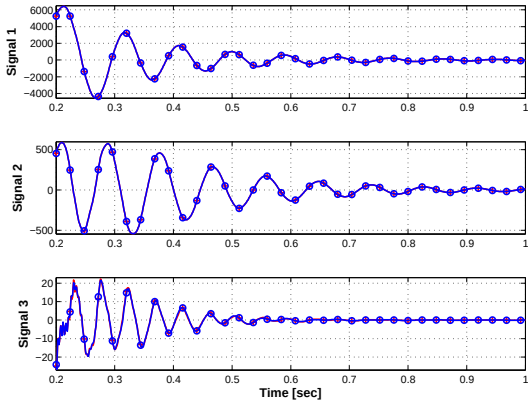

Figure 4: Curve fitting of the optimized signals (v_n =500 ft/s). Original signal (+) and reconstructed signal ($\circ$).

between the optimized signal and its reconstructed counterpart. The error measures were found to be $\epsilon_1 = 0.15\%$, $\epsilon_2 = 0.4\%$ and $\epsilon_3 = 0.35\%$ for the first three signals depicted in fig. 4. Clearly, for a far field flow velocity v_n =500 ft/s, stability characteristics are estimated accurately from the optimized signals.

4.2 Simply supported beam under parametric excitation

The second example deals with the parametric excitation of a simply supported beam. Figure 5 shows the uniform beam of length $L = 1$ m, bending stiffness $EI = 6.57$ kN·m^2, and mass per unit span, $m = 3.24$ kg/m, subjected to an axial compressive load $P = P_0 + P_1 \cos(\omega_p t)$.

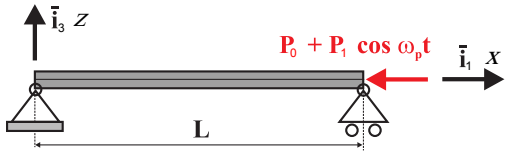

Figure 5: Parametric excitation of a simply supported beam.

Based on the Euler-Bernoulli assumptions, the

governing equation for the beam is

$$EI\frac{\partial^4 w}{\partial x^4} + (P_0 + P_1 \cos\omega_p t)\frac{\partial^2 w}{\partial x^2} + c\frac{\partial w}{\partial t} + m\frac{\partial^2 w}{\partial t^2} = 0, \tag{24}$$

where w is the transverse displacement and c the damping coefficient. This equation is solved via separation of variables [22] by assuming the following expression for transverse displacement field

$$w(x,t) = q_k(t)\sin\frac{k\pi x}{L}, \quad k = 1, 2, \ldots, n. \tag{25}$$

Introducing this expression into the governing equation (24) leads to

$$\ddot{q}_k + \epsilon\dot{q}_k + \omega_k^2(1 - 2\mu_k\cos\omega_p t)q_k = 0. \tag{26}$$

The k^{th} natural frequency and Euler buckling load of the beam are denoted Ω_k and P_k, respectively, and the following notation was introduced

$$\begin{aligned} \Omega_k &= \frac{k^2\pi^2}{L^2}\sqrt{\frac{EI}{m}}, \quad P_k = \frac{k^2\pi^2 EI}{L^2}, \quad \epsilon = \frac{c}{m}, \\ \omega_k &= \Omega_k\sqrt{1 - \frac{P_0}{P_k}}, \quad \mu_k = \frac{1}{2}\,\frac{P_1}{P_k - P_0}. \end{aligned} \tag{27}$$

Equation (26) shows that the beam's stiffness varies harmonically with a period, $T = 2\pi\omega_p$, equal to that of the axial excitation.

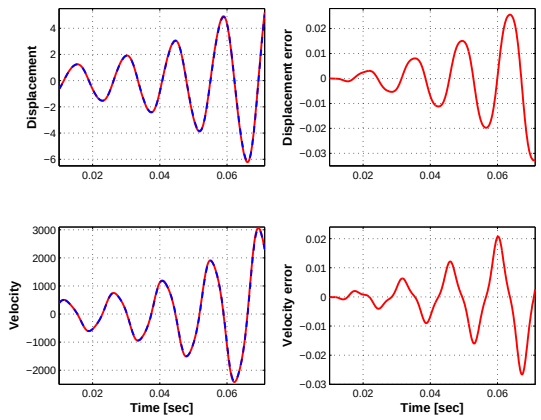

Figure 6: Time histories of q_1 (top figure) and $\dot{q}_1$ (bottom figure) for ODE45 (solid line) and the exponential approximation (dashed line). Figures on the right show the normalized error between the two prediction.

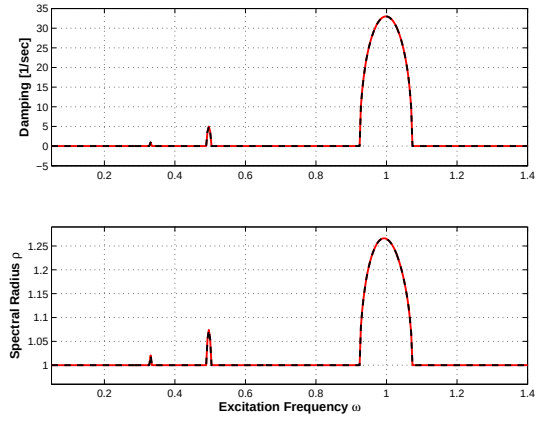

Figure 7: Damping (top figure) and spectral radius (bottom figure) of the dominant eigenvalue of the system versus excitation frequency, for $\mu = 0.15$. Floquet classical analysis: solid line; present approach by MatLab: dashed line.

The proposed approach is based on the evaluation of the LCEs and relies on the exponential approximation expressed by eq. (15). To validate this approach, equation (26) is solved first with the high-accuracy routine ODE45 implemented in MATLAB then with the proposed exponential approximation (15). The following parameters were used in eq. (26): $k = 1$, $\epsilon = 0$, $\mu_1 = 0.15$, $\omega_p = 2\omega_1$, $q_1(t = 0) = 1$, and $\dot{q}_1(t = 0) = 1$. Figure 6 shows the results for the two integration methods together with the error incurred by the exponential approximation; the error is evaluated as the difference between the two integration procedures, normalized by the maximum value of the corresponding quantity. Clearly, the exponential approximation is very accurate in this case.

Next, the proposed LCEs approach was used to identify the stability characteristics of the undamped beam modeled by eq. (26) and using the values of the parameters given above. Figure 7 depicts the stability characteristics (real part and norm of the dominant Floquet characteristic exponent) as functions of the excitation frequency, $\omega = \omega_p/(2\omega_k)$. For reference, the predictions of the classical Floquet theory [1] are also shown: the predictions of the two approaches are in excellent agreement.

To further validate the proposed approach, the same beam was modeled using the finite element method. The model consists of geometrically exact beams and two revolute joints; the beam was modeled with four cubic beam elements and the complete index-3 differential algebraic equations had a total of 77 dofs. Structural damping was modeled by incorporating viscous forces proportional to the strain rates, $\underline{F}_d = \nu_s \underline{\underline{K}}_s \underline{\dot{e}}$, where ν_s is the damping coefficient, $\underline{e}$ is the array of sectional strains, and $\underline{\underline{K}}_s$ is the beam cross-sectional stiffness matrix. The damping coefficient was selected as $\nu_s = 2 \times 10^{-4}$ s, which is equivalent to $\epsilon = 40.56$ s^{-1} in eq. (26). All other parameters remain unchanged.

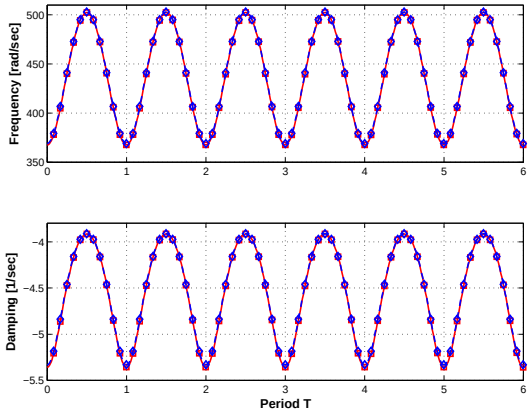

Figure 8: Time history of natural frequency (top figure) and structural damping (bottom figure) for $\epsilon = 40.56$. Floquet classical analysis: solid line (□); proposed approach: dashed line (◇).

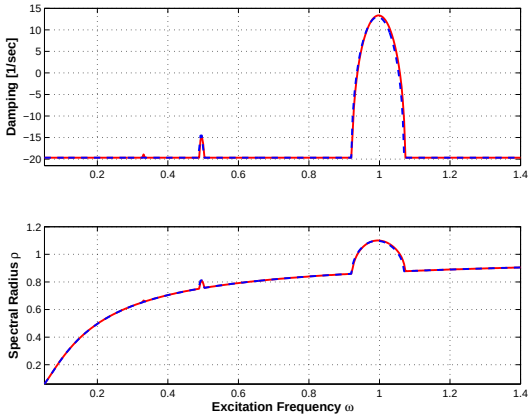

Figure 9: Damping (top figure) and norm (bottom figure) of the maximum eigenvalue of the system versus excitation frequency, for $\epsilon = 40.56$. Floquet classical analysis: solid line; present approach: dashed line.

Because the problem is periodic, the instantaneous stability characteristics are now functions of time, as depicted in fig. 8, which shows the characteristics associated with the dominant mode. The stability behavior of the system cannot be predicted from this data directly. In fact, the time traces shown in fig. 6 seem to indicate that the system is unstable.

To assess stability, modal reduction is performed and the solution of the reduced system is obtained from the exponential approximation (15), leading to the reduced transition matrix, $\underline{\underline{\hat{Q}}}$. The eigenvalues of this matrix provide the desired stability characteristics (real part and spectral radius of dominant eigenvalue of $\underline{\underline{\hat{Q}}}$) shown in fig. 9. For reference, the predictions of the classical Floquet theory applied to equation (26) are also shown. Once again, a good correlation is observed between the two approaches. A small zone of instability is identified for $0.9357 < \omega < 1.0540$; the results presented in fig. 6 correspond to $\omega_p = 2\omega_1$, where the system is unstable.

5 Conclusions

Two time domain approaches to the stability analysis of flexible dynamical systems are proposed in this paper. The first is based on partial Floquet theory and proceeds in three steps. A pre-

processing step evaluates optimized signals based on the proper orthogonal decomposition method. Next, the system stability characteristics are obtained from partial Floquet theory through singular value decomposition. Finally, a postprocessing step assesses the accuracy of the identified stability characteristics.

The Lyapunov characteristic exponent theory provides the theoretical background for the second approach. The relationship between system eigenvalues and the LCEs have been identified for both constant and periodic coefficient systems. For constant coefficient systems, the LCEs are identical to the eigenvalue of the system and can be determined directly from eigenvalues decomposition. For periodic system, the LCEs equal the real parts of eigenvalues of the transition matrix, which is evaluated through the proposed exponential approximation.

The flutter speed of a rectangular planform wing was predicted based of the two proposed approaches and compared favorably with experimental results. Next, the parametric excitation of simply supported beam was investigated. The predictions of the proposed approach were found to be in close agreement with those of the classical Floquet method. These numerical examples demonstrate that the proposed approaches are robust enough to deal with the stability analysis of dynamical systems in an efficient manner.

References

[1] H. Hochstadt. *Differential Equations*. Dover Publications, Inc., New York, 1964.

[2] A.H. Nayfeh and D.T. Mook. *Nonlinear Oscillations*. John Wiley & Sons, New York, 1979.

[3] X. Wang. The method of generalized Floquet theory applied to flap-lag dynamics with inflow. Master's thesis, Washington University, Saint Louis, 1998.

[4] O.A. Bauchau and J.L. Wang. Stability evaluation and system identification of flexible multibody systems. *Multibody System Dynamics*, 18(1):95–106, October 2007.

[5] O.A. Bauchau and J.L. Wang. Efficient and robust approaches for rotorcraft stability analysis. *Journal of the American Helicopter Society*, 55:012005 1–12, 2010.

[6] F.E. Udwadia and H.F. von Bremen. Computation of Lyapunov characteristic exponents for continuous dynamical systems. *Zeitschrift für angewandte Mathematik und Physik*, 53(1):123–146, 2002.

[7] K. Geist, U. Parlitz, and W. Lauterborn. Comparison of different methods for computing Lyapunov exponents. *Progress of Theoretical Physics*, 83(5):875–893, 1990.

[8] O.A. Bauchau and J.L. Wang. Efficient and robust approaches to the stability analysis of large multibody systems. *Journal of Computational and Nonlinear Dynamics*, 3(1):011001 1–12, January 2008.

[9] O.A. Bauchau. *Flexible Multibody Dynamics*. Springer, Dordrecht, Heidelberg, London, New-York, 2011.

[10] J. Wang and Z. Li. Implementation of HHT algorithm for numerical integration of multibody dynamics with holonomic constraints. *Journal of Nonlinear Dynamics*, 24(6):983–990, June 1986.

[11] G.H. Golub and C.F. van Loan. *Matrix Computations*. The Johns Hopkins University Press, Baltimore, second edition, 1989.

[12] W.E. Arnoldi. The principle of minimized iterations in the solution of the matrix eigenvalue problem. *Quarterly of Applied Mathematics*, 9:17–29, 1951.

[13] A. Wolf, Swift J.B., H.L. Swinney, and J.A. Vastano. Determining Lyapunov exponents from a time series. *Physica D: Nonlinear Phenomena*, 16(3):285–317, 1985.

[14] M. Goland. The flutter of a uniform cantilever wing. *Journal of Applied Mechanics*, 12(4):A197–A208, 1945.

[15] J. Wang. Implementation of geometrically exact beam element for nonlinear dynamics modeling. *Multibody System Dynamics*, 1(1):1–16, April 2015.

[16] E.C. Yates. Calculation of flutter characteristics for finite-span swept or unswept wings at subsonic and supersonic speeds by a modified strip analysis. Technical Report RM L57L10, NACA Research Memorandum, 1958.

[17] J.G. Barmby, H.J. Cunningham, and I.E. Garrick. Study of effects of sweep on the flutter of cantilever wings. Technical Report NR 1014, NACA Report, 1951.

[18] R. Theodorsen. General theory of aerodynamic instability and the mechanism of flutter. Technical Report 496, NACA Report, 1949.

[19] J.O. Scherer. Experimental and theoretical investigation of large amplitude oscillation foil propulsion systems. Technical report, U.S. Army Engineering Research and Development Laboratories, 1968.

[20] J.D. Delaurier and J.M. Harris. An aerodynamic model for flapping-wing flight. *The Aeronautical Journal of the Royal Aeronautical Society*, 97(964):125–140, April 1993.

[21] J. Wang, J. Rodriguez, and R. Keribar. Integration of flexible multibody systems using Radau IIA algorithms. *Journal of Computational and Nonlinear Dynamics*, 5(4):041008–14 pages, 2010.

[22] V.V. Bolotin. *Nonconservative Problems of the Theory of Elastic Stability*. Pergamon Press Limited, Oxford, England, 1963.